# Effects of Amiodarone on Ventricular Excitation associated with the KCNJ2-Linked Short QT Syndrome: Insights from a Modelling Study

Cunjin Luo[1], Kuanquan Wang[1], Ming Yuan[2], Zhili Li[2], Qingjie Wang[3],
Yongfeng Yuan[1], Qince Li[1], Henggui Zhang[1,4]

[1]School of Computer Science and Technology, Harbin Institute of Technology, Harbin, China
[2]State Key Lab of Space Medicine Fundamentals and Application, China Astronaut Research and Training Center, Beijing, China
[3]Department of Cardiology, Zhongda Hospital of Southeast University, Nanjing, China
[4]School of Physics and Astronomy, the University of Manchester, Manchester, UK

## Abstract

*Short QT syndrome (SQTS) is associated with ventricular arrhythmias that may lead to cardiac sudden death. However, effective pharmacological treatment for SQTS remains unclear. Amiodarone has emerged as the leading antiarrhythmic therapy for termination and prevention of ventricular arrhythmia in different clinical settings because of its proven efficacy and safety. The aim of this study was to investigate the effects of amiodarone on cardiac excitation of the KCNJ2-linked short QT syndrome. Effects of Kir2.1 D172N mutation-induced changes in $I_{K1}$ were incorporated into human ventricular cell and tissue models that considered the intrinsic electrical heterogeneity in the left ventricle. Actions of amiodarone were simulated by implementing a simple block pore theory to simulate the drug's effects on $I_{CaL}$ and $I_{Kr}$ block for several doses. In cellular simulations, current traces of $I_{Kr}$ and $I_{CaL}$ and action potential duration of ENDO, M, and EPI cells were simulated in control, mutant, and amiodarone-in-action conditions. In tissue simulations, the pharmacological effects of amiodarone on the characteristics of ECG were examined. This study provides new insights into the pharmacokinetics of amiodarone for treatment of SQT3 under WT-D172N and D172N conditions.*

## 1. Introduction

The short QT Syndrome (SQTS) is a recently identified cardiac disease associated with short QT intervals on the ECG and with an increased risk of malignant ventricular arrhythmias and of sudden cardiac death (SCD) [1~3]. SQT3 is identified as a genetic mutation, in which aspartic acid is replaced by asparagines at position 172 in the Kir2.1 potassium channel [4]. El Harchi et al. [5] have shown the Kir2.1 D172N mutation resulted in preferential augmentation of the outward current.

Currently in SQTS patients, the first-line treatment and prophylactic therapy is the use of implantable cardioverter defibrillators (ICDs), which can help to prevent episodes of ventricular fibrillation, but the use of ICDs carries an increased risk of an inappropriate shock discharge by the ICD due to T-wave over-sensing [6,7]. ICDs do not restore the QT interval to its normal duration and are not suitable for the young patients [7]. Therefore, pharmacological therapy may be the primary modality to restore the normal QT interval and protect against arrhythmias [6, 8].

At present, due to the scarcity of accurate experimental models of SQT3 and in vitro pharmacological data of SQT3, silico models provide a complementary method to characterize and quantify the effects of channel-blocking drug targeting SQT3 mutation. Amiodarone, class III anti-arrhythmic, is known to prolong the QT interval, and is an effective drug for the treatment of atrial and ventricular arrhythmias in patients for termination and prevention of ventricular arrhythmia in different clinical settings.

In the present computational study, the dose-dependent effects of amiodarone on cardiac electrophysiological properties were examined. Furthermore, the impact of amiodarone on the pseudo-ECG was investigated. Therefore, this study provides a better assessment of the pharmacological effects and adverse effects of amiodarone.

## 2. Materials and methods

### 2.1. Modelling drug-channel interaction

The effect of drug on blocking an ion channel can be simulated using a blocking factor k that reduces the

maximum conductance of the targeted ion channel. Mathematically, k is expressed as:

$$k = \frac{1}{1 + (\frac{[D]}{IC_{50}})^{nH}} \quad (1)$$

where $[D]$ is the drug concentration, $IC_{50}$ is the drug concentration of 50% blockade of the binding site and $nH$ is the Hill coefficient.

To simulate the actions of amiodarone, we used the simple pore block theory, by which the maximal channel conductance of the targeted channel(s) was reduced by various percentages according to the dose of the amiodarone (as shown in Table 1). For example, the channel conductances of $I_{Kr}$ and $I_{CaL}$ were reduced to 42.8 and 85.3%, respectively, for 1 μM amiodarone [9,10].

Table 1 Reduction of ion channel conductivities (% of original value) due to amiodarone

| | Amiodarone | | | | | |
|---|---|---|---|---|---|---|
| | 7μM | 5μM | 3μM | 1μM | 0.8μM | 0.6μM |
| $G_{CaL}$ | 44.8% | 54.4% | 65.9% | 85.3% | 87.6% | 90.4% |
| $G_{Kr}$ | 4.9% | 7.7% | 15.2% | 42.8% | 49.1% | 60.2% |

## 2.2. Cardiac models of human ventricular cells

In this section, we used the ten Tusscher, Noble, Noble and Panfilov (TNNP) mathematical models to simulate human ventricular APs [11]. These models reproduce electrical properties and transmural AP heterogeneity of human ventricle. The electrophysiological behavior of a single cell is described as following:

$$\frac{\partial V_m}{\partial t} = -\frac{I_{ion} + I_{stim}}{C_m} \quad (2)$$

where $V_m$ is transmembrane potential, $C_m$ is the membrane capacitance, $I_{stim}$ is the externally applied stimulus current, $t$ is time, $I_{ion}$ is the sum of ionic currents as described in the following equation:

$$I_{ion} = I_{Kr} + I_{Ks} + I_{K1} + I_{to} + I_{Na} + I_{bNa} + I_{CaL}$$
$$+ I_{bCa} + I_{NaK} + I_{NaCa} + I_{pCa} + I_{pK} + I_{NaL} \quad (3)$$

For the present study, mathematical equations of IK1 were modified for three main situations: WT, WT-D172N and D172N, which are described as follows [12]:

$$I_{k1} = G_{k1} \sqrt{\frac{K_o}{5.4}} x_{k1\infty}(V - E_k) \quad (4)$$

$$x_{k1\infty} = \frac{\alpha_{k1}}{\alpha_{k1} + \beta_{k1}} \quad (5)$$

WT:

$$\alpha_{k1} = \frac{0.07}{1 + e^{0.017(V - E_k - 200.2)}} \quad (6)$$

$$\beta_{k1} = \frac{3e^{0.0003(V - E_k + 100.2)} + e^{0.08}(V - E_k - 8.7)}{1 + e^{-0.024(V - E_k)}} \quad (7)$$

$$G_{k1} = 4.8 ns/pF \quad (8)$$

WT-D172N:

$$\alpha_{k1} = \frac{0.1}{1 + e^{0.023(V - E_k - 199.9)}} \quad (9)$$

$$\beta_{k1} = \frac{3e^{0.0002(V - E_k + 100.4)} + e^{0.07(V - E_k - 9.8)}}{1 + e^{-0.02(V - E_k)}} \quad (10)$$

$$G_{k1} = 6.27 ns/pF \quad (11)$$

D172N:

$$\alpha_{k1} = \frac{0.1}{1 + e^{0.05(V - E_k - 199.9)}} \quad (12)$$

$$\beta_{k1} = \frac{3e^{0.0002(V - E_k + 100.1)} + e^{0.08(V - E_k - 10.3)}}{1 + e^{-0.006(V - E_k)}} \quad (13)$$

$$G_{k1} = 11.32 ns/pF \quad (14)$$

where $G_{k1}$ is the maximal conductance of $I_{k1}$, $x_{k1\infty}$ is the time-independent inward rectification factor.

## 2.3. Computing the pseudo-ECG

The pseudo-ECG was calculated as an integral of gradient of membrane potential at all positions in the tissue from a virtual electrode located in the extracellular space used by other studies [12-14], which was described as following:

$$\Phi = \int \frac{D \nabla V_m \cdot \vec{r}}{r^3} dV \quad (15)$$

where $\Phi$ is electrical potential, $V$ is the area of 2D tissue. $\vec{r}$ is the vector from the recording electrode to a point in the tissue. In this study, we placed the virtual electrode in the middle of the model at the left side, 2 cm distance off the cells. 2D model comprised Purkinje fiber region (cells 40 × (1~50)), ventricle region (cells 40 × (51~150)). 2D simulations were carried out in an isotropic domain with D=0.1, with a time step of 0.02 ms and a space step of 0.2 mm. These equations were solved using the forward Euler method.

## 3. Results

At first, in cellular simulations, the impacts of amiodarone on isolated control and SQT3 ventricular cells were investigated. We simulated current traces of $I_{CaL}$ and $I_{Kr}$ in both control and amiodarone-in-action conditions. The time courses of $I_{CaL}$ and $I_{Kr}$ for ENDO, M, and EPI cells in WT, amiodarone-in-actions are shown in

Fig. 1. 1µM and 7µM doses of amiodarone effects of ENDO, M, and EPI APs under the KCNJ2-linked short QT syndrome were shown in Fig. 2. Fig. 3 shows $APD_{90}$ histogram of the different doses of amiodarone on ventricular excitation associated with KCNJ2-linked short QT syndrome. Simulation results suggested that both high- and low- dose of amiodarone did not markedly affect the AP amplitude, resting potential, but significantly altered $APD_{90}$ under the KCNJ2-linked short QT syndrome condition. As compared to WT condition, amiodarone prolonged action potential slightly in M cells, but insignificantly at low dose in ENDO and EPI cells.

The effects of amiodarone on the characteristics of a pseudo-ECG were shown in Fig.4. In simulations, amiodarone did not change the QRS complex. The high dose of amiodarone shortened the QT interval significantly under both WT-D172N and D172N conditions. However, low dose of amiodarone only shortened the QT interval under D172N condition and did not induce noticeable effect on the QT interval under WT-D172N condition.

## 4. Discussion

In this study, we delineated the effects of amiodarone on cardiac excitation associated with KCNJ2-linked short QT syndrome using a computational method. For this purpose, different dose-dependent inhibitory effects of amiodarone were integrated into a model of WT and SQT3 ventricular myocytes. The impacts of amiodarone on cardiac electrophysiology and ECGs were investigated. These computational simulations help to better understand the pharmacological effects of amiodarone, which provides new insights into the pharmacokinetics of amiodarone for treatment of SQT3 under WT-D172N and D172N conditions.
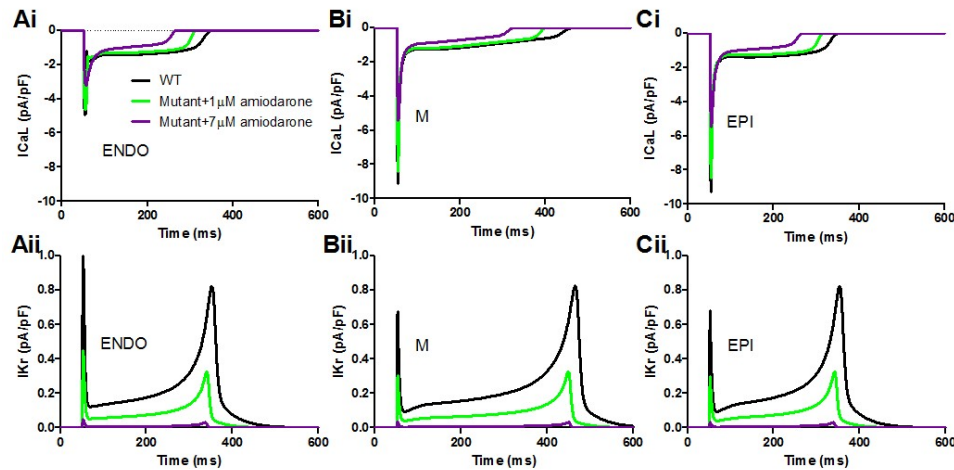
## Acknowledgements

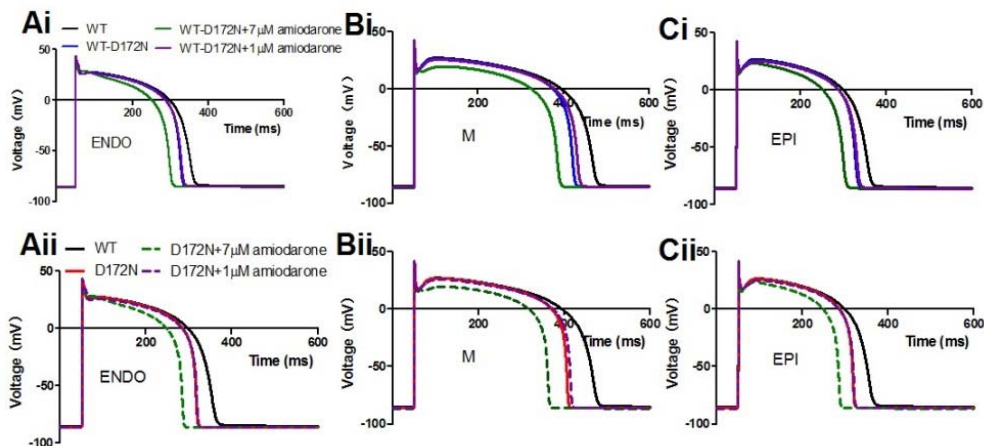Fig. 1. Plots of $I_{CaL}$ and $I_{Kr}$ currents in WT, mutant and amiodarone-in-action conditions

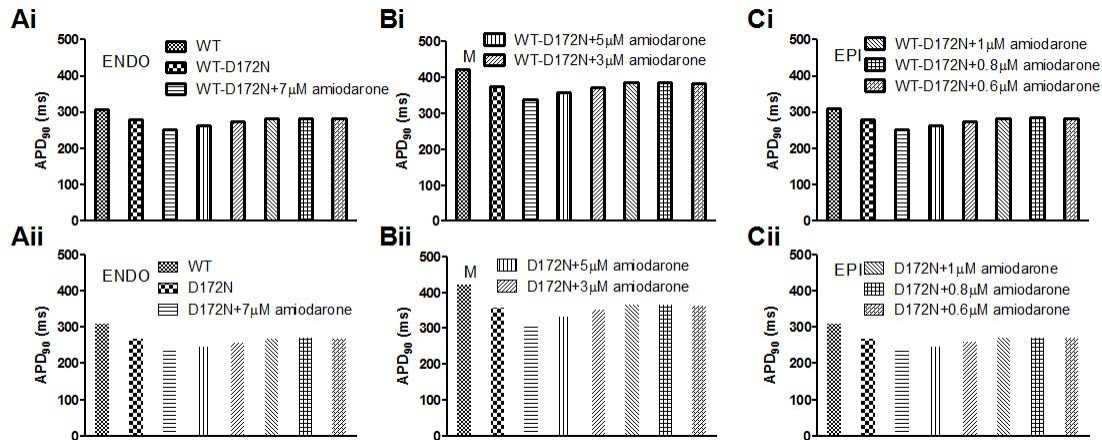Fig. 2. Plots of action potentials in WT, mutant and amiodarone-in-action conditions



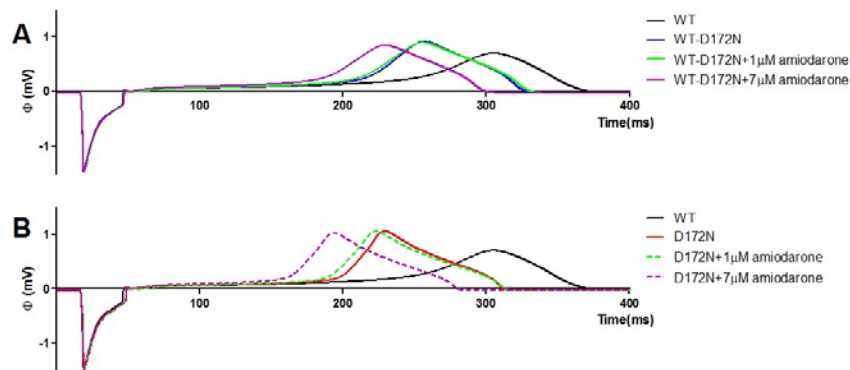Fig. 3. Histogram comparison of APD$_{90}$ in WT, mutant and amiodarone-in-action conditions



Fig. 4. Computed pseudo-ECG in WT, mutant and amiodarone-in-action conditions

# References

[1] Gussak I, Brugada P, Brugada J, et al. Idiopathic short QT interval: a new clinical syndrome? Cardiology 2000;94:99-102.

[2] Gaita F, Giustetto C, Bianchi F, et al. Short QT syndrome: a familial cause of sudden death. Circulation, 2003; 108: 965-970.

[3] Schimpf R, Wolpert C, Gaita F, et al. Short QT syndrome. Cardiovasc Res, 2005; 67: 357-366.

[4] Priori, SG, Pandit SV, Rivolta I, Berenfeld O, Ronchetti E, Dhamoon A, Napolitano C, Anumonwo J, Di Barletta MR, Gudapakkam S, Bosi G, Stramba-Badiale M &Jalife J.A novel form of short QT syndrome (SQT3) is caused by a mutation in the KCNJ2 gene. Circ Res 2005; 96: 800-7.

[5] EL Harchi A, Mcpate MJ, Zhang Y, Zhang H &Hancox JC. Action potential clamp and chloroquine sensitivity of mutant Kir2.1 channels responsible for variant 3 short QT syndrome. J Mol Cell Cardiol 2009; 47: 743-7.

[6] Schimpf R, Wolpert C, Gaita F, Giustetto C, Borggrefe M. Short QT syndrome. Cardiovasc Res, 2005; 67: 357-366.

[7] Schimpf R, Wolpert C, Bianchi F, Giustetto C, Gaita F, et al. Congenital short QT syndrome and implantable cardioverter defibrillator treatment: inherent risk for inappropriate shock delivery. J Cardiovasc Electrophysiol, 2003; 14: 1273-1277.

[8] Bjerregaard p, Jahangir A, et al. Targeted therapy for the short QT syndrome. Expert Opin Ther Targets, 2006; 10: 393-400

[9] Nishimura M et al, et al. Amiodarone blocks calcium current in single guinea pig ventricular myocytes. J Pharmacol Exp Ther, 1989; 251: 650-659.

[10] Wu L et al. Augmentation of late sodium current unmasks the proarrhythmic effects of amiodarone. Cardiovasc Res, 2008; 77: 481-488.

[11] Ten Tusscher KH &Panfilov AV. Alternans and spiral breakup in a human ventricular tissue model. Am J Physiol Heart CircPhysiol 2006; 291: H1088-100.

[12] Adeniran I, EL Harchi A, Hancox JC & Zhang H. Proarrhythmia in KCNJ2-linked short QT syndrome: insights from modelling. Cardiovasc Res 2012; 94: 66-76.

[13] Wang K, Luo C, Wang W, Zhang H, Yuan Y. Simulation of KCNJ2-linked short QT syndrome in human ventricular tissue. Computing in cardiology 2013; 40: 349-352.

[14] Wang K, Luo C, Yuan Y, Lu W, Zhang H. Simulation of re-entrant wave dynamics in a 2-D sheet of human ventricle with KCNJ2-linked variant 3 short QT syndrome. Computing in Cardiology 2014; 41: 61-64.

Kuanquan Wang (wangkq@hit.edu.cn)
Mailbox 332, Harbin Institute of Technology, Harbin, China.